Ecosystems (2024) 27: 1–18
https://doi.org/10.1007/s10021-023-00868-8

ECOSYSTEMS

ORIGINAL ARTICLE

Effect of Drought and Heavy Precipitation on CH_4 Emissions and $\delta^{13}C–CH_4$ in a Northern Temperate Peatland

Clarice R. Perryman,[1,2,3]* Carmody K. McCalley,[4] Joanne H. Shorter,[5] Apryl L. Perry,[2,3] Natalie White,[6] Angelica Dziurzynski,[2,7,8] and Ruth K. Varner[2,3]

[1]*Department of Earth System Science, Stanford University, Stanford, California, USA;* [2]*Department of Earth Sciences, University of New Hampshire, Durham, New Hampshire, USA;* [3]*Institute for the Study of Earth, Oceans, and Space, University of New Hampshire, Durham, New Hampshire, USA;* [4]*Thomas H. Gosnell School of Life Sciences, Rochester Institute of Technology, Rochester, New York, USA;* [5]*Aerodyne Research Inc., Billerica, Massachusetts, USA;* [6]*Department of Natural Resources and the Environment, University of New Hampshire, Durham, New Hampshire, USA;* [7]*Department of Biological Sciences, University of New Hampshire, Durham, New Hampshire, USA;* [8]*Department of Marine Sciences, University of Georgia, Athens, Georgia, USA*

Abstract

Shifting precipitation patterns due to climate change may impact peatland methane (CH_4) emissions, as precipitation affects water table level which largely controls CH_4 cycling. To investigate the impact of variable precipitation on peatland CH_4 emissions, we measured CH_4 fluxes and their ^{13}C isotope composition ($\delta^{13}C–CH_4$) across two summers marked by drought (2020) and heavy precipitation (2021) in a northern temperate poor fen in New Hampshire, USA. Monthly variation in CH_4 fluxes and $\delta^{13}C–CH_4$ was larger than interannual variation and variation between peatland microforms. While the seasonal pattern of CH_4 emissions was not significantly different between years, the magnitude of seasonal changes in CH_4 flux and $\delta^{13}C–CH_4$ provided insight regarding the processes controlling CH_4 emissions. Between July and August 2020, water table levels dropped > 15 cm, CH_4 emissions decreased by an order of magnitude, and $\delta^{13}C–CH_4$ increased $\sim 10‰$, suggesting lower water table levels promoted CH_4 oxidation and reduced emissions in late summer. Rainstorms in July 2021 caused flooding and stimulated high CH_4 emissions, but the impact of increased water table levels due to heavy precipitation on CH_4 fluxes was transient and did not have an apparent effect on emitted $\delta^{13}C–CH_4$. While drought conditions had a clear impact on CH_4 fluxes and $\delta^{13}C–CH_4$, our results suggest rainstorms and subsequent flooding do not have a sustained impact on CH_4 emissions from temperate peatlands.

Key words: Methane emissions; Peatlands; Wetlands; Stable isotopes; Drought; Precipitation; Methanogenesis; Methanotrophy.

Received 25 January 2023; accepted 19 July 2023; published online 9 August 2023

Supplementary Information: The online version contains supplementary material available at https://doi.org/10.1007/s10021-023-00868-8.

Author Contributions: CRP, CKM, and RKV conceived of the study design. RKV and CRP secured funding for the research. CKM, JS, and AP made significant contributions to the stable isotope analytical methods. CRP, AP, NW, AD, and RKV conducted fieldwork and laboratory analyses. CRP analyzed the data and wrote the manuscript. All other authors provided feedback on draft manuscript materials.

**Corresponding author; e-mail:* crperry@stanford.edu

Highlights

- Methane fluxes and $\delta^{13}C$–CH_4 varied more by month than by year or microtopography
- Drought decreased CH_4 fluxes and increased $\delta^{13}C$–CH_4, indicating high CH_4 oxidation
- Rainstorms and flooding briefly increased CH_4 fluxes but had no effect on $\delta^{13}C$–CH_4

Introduction

Peatlands north of 40°N are globally significant carbon (C) stores (Yu and others 2012) and methane (CH_4) sources (Crill and others 1988; Treat and others 2018). Accelerated warming and shifts in precipitation due to anthropogenic climate change are driving interacting changes in peatland hydrology (Waddington and others 2015), vegetation (Breeuwer and others 2009; Camill 1999), and microbial communities (Peltoniemi and others 2016; Wilson and others 2021) that will impact CH_4 emissions from northern peatlands. It is well established that increasing temperatures generally lead to increased peatland CH_4 emissions (for example, Christensen and others 2003; Hopple and others 2020), pending coincident changes in hydrology. At the landscape level, sites with higher water table levels are also generally associated with higher CH_4 emissions (for example, Bubier and others 1993; Kuhn and others 2021; Segers 1998), but the relationship between water table and CH_4 fluxes is often mediated by other peatland characteristics including vegetation cover and nutrient status (Turetsky and others 2014).

At the site-level, interannual variability in precipitation can have a large impact on both water table level and CH_4 emissions. In general, CH_4 emissions from the same site are larger in years with greater cumulative precipitation during the growing season (Bubier and others 2005; Olson and others 2013), as precipitation partially regulates water table position and delivers thermal energy to the subsurface that promotes methanogenesis (Neumann and others 2019; Olefeldt and others 2017). Beyond cumulative precipitation, shifts in the intensity and/or frequency of precipitation can cause large variability in peatland CH_4 emissions by disrupting water table dynamics (Barel and others 2021; Radu and Duval 2018). Much of the prior research on changing water table levels and CH_4 emissions in northern peatlands has focused on predicted long-term changes like drying due to warmer temperatures and increased evapotranspiration or flooding due to permafrost thaw in high latitude sites (for example, Roulet and others 1992; Strack and others 2004; Turetsky and others 2008), rather than interannual differences in precipitation patterns. As precipitation patterns are expected to change in their seasonality and intensity under warmer climate (Douville and others 2021), further work is needed to understand the impact of more variable precipitation on peatland CH_4 emissions. This is particularly important in permafrost-free peatlands where shifting precipitation patterns will play a larger role in controlling hydrologic conditions and CH_4 emissions under a changing climate.

Furthermore, there is a need to better characterize the underlying mechanisms that determine how peatland CH_4 emissions will respond to changing precipitation patterns. Measurements of the stable isotopic composition of CH_4 ($\delta^{13}C$–CH_4) could help provide this insight, as characteristic isotope fractionation patterns of methanogenesis, methanotrophy, and gas transport enable the use of $\delta^{13}C$–CH_4 measurements to make inferences about dominant processes. Methane is produced by methanogenic archaea via two dominant processes: acetoclastic methanogenesis (the fermentation of acetate into CH_4 and CO_2) and hydrogenotrophic methanogenesis (the reduction of H_2 with CO_2). Acetoclastic methanogenesis produces CH_4 with higher $\delta^{13}C$–CH_4 than hydrogenotrophic methanogenesis (−70 to −30‰ vs. −100 to −60‰; Whiticar 1999). As such, seasonal changes in $\delta^{13}C$–CH_4 have previously been linked to changes in dominant methanogenic pathway in response to increasing plant productivity (Avery and others 1999) or temperature across the growing season (Wilson and others 2021). Methane oxidation leaves residual CH_4 enriched in ^{13}C (Coleman and others 1981), yielding larger $\delta^{13}C$–CH_4 values. Therefore, shifts in $\delta^{13}C$–CH_4 coincident with changing in water table levels may indicate changes in rates of aerobic CH_4 oxidation (Kelly and others 1992). Considering the impact of gas transport on $\delta^{13}C$–CH_4 may further elucidate drivers of CH_4 fluxes. Plant mediated transport through aerenchyma in sedges (for example *Carex spp.* and *Eriophorum spp.)* results in greater emissions of $^{12}CH_4$ relative to $^{13}CH_4$, decreasing $\delta^{13}C$–CH_4 values ~ 5–10‰, whereas ebullition and diffusion across the water–air interface have negligible effects on $\delta^{13}C$–CH_4 (≤ 1‰; Chanton, 2005). As such, if drought were to drop water table levels below the rhizosphere in sedge-dominated peatlands $\delta^{13}C$–CH_4 could increase substantially as plant-mediated transport may be inhibited alongside a potential increase in CH_4 oxidation (Popp and others 1999).

Prior $\delta^{13}C–CH_4$ measurements from studies of peatland drought and rewetting cycles suggest that changing precipitation patterns will have less influence on methanogenic pathways than on methanotrophy (Knorr and others 2008a), and that the effect of drought conditions on CH_4 cycling depends on interactions with temperature and peatland type (White and others 2008). However, these insights come from mesocosm experiments which do not fully recreate field-relevant conditions and processes, and more field-based observations of how $\delta^{13}C–CH_4$ changes in response to variable precipitation patterns are needed. Few field-based studies have examined how events like droughts or rainstorms and subsequent flooding affect $\delta^{13}C–CH_4$. Beyond providing insights into mechanisms controlling the response of CH_4 emissions to variable precipitation, such measurements could help improve CH_4 source partitioning by global atmospheric models which are highly sensitive to spatiotemporal variation of source $\delta^{13}C–CH_4$.

In this study, we aimed to resolve the impact of variable precipitation on the source $\delta^{13}C–CH_4$ signature of peatland CH_4 emissions, and in turn use observations of $\delta^{13}C–CH_4$ to identify mechanisms driving the response of CH_4 emissions to drought and flooding. We measured CH_4 fluxes and $\delta^{13}C–CH_4$ in a well-studied northern temperate peatland across one summer characterized by drought and a falling water table and one summer characterized by rainstorms and flooding. Our measurements were conducted across collars that varied in water table depth and dominant vegetation to assess if the differing precipitation and water table dynamics had similar impacts on CH_4 cycling across the landscape. We hypothesize that (1) the differing precipitation and water table conditions would result in overall lower CH_4 fluxes and higher $\delta^{13}C–CH_4$ values in the dry year and (2) seasonal variation in CH_4 fluxes and $\delta^{13}C–CH_4$ would differ between years, as flooding or drying across the growing season alternatively promote CH_4 production and oxidation, respectively.

Materials and Methods

Study Setting: Field Site and Precipitation Conditions

Measurements were conducted at Sallie's Fen (43°12.5′N, 71°3.5′W), a mineral-poor fen located in Barrington, New Hampshire, USA. The growing season extends from late April to October, with deciduous plant senescence beginning in September. Vegetation at Sallie's Fen is dominated by moss (primarily *Sphagnum* spp.), and dominant vascular vegetation includes ericaceous shrubs (for example *Chamaedaphne calyculata, Vaccinium oxycoccos,* and *V. corymbosum*), sedges (*Carex rostrata*), herbaceous perennials (for example, *Eurybia radula, Maianthemum trifolium),* and deciduous shrubs (*Alnus incana spp. rugosa*) and trees (*Acer rubrum*).

We collected measurements from mid-May to late August 2020–21 from 10 long-term static flux collars. The collars were grouped into 3 microforms based on their vegetation composition and water table depth (Figure S1, Table S1): hummock (n = 4), lawn (n = 3), and wet (n = 3). In hummocks, the ground surface was 10 to 20 cm above the surrounding peat outside of the collar area. The wet microforms are not depressions and/or hollows, but rather areas of the study site where surface water preferentially pools throughout the growing season. Vegetation communities were also distinct between the 3 microforms (Figure S1A). Lawns had the highest proportion of sedge cover of the 3 microforms (ANOVA, $F_{2,7} = 16.5$, $p = 0.002$; Figure S1B). Hummocks and lawns also had a higher proportion of shrubs than wet microforms ($F_{2,7} = 36.9$, $p < 0.001$).

Sallie's Fen receives water primarily through precipitation, with secondary inputs from run-off and an ephemeral stream that bounds the northern edge of the site. Mean seasonal water table depth from May to August is approximately 10–25 cm below the peat surface (Noyce and others 2014; Treat and others 2007). The water table position usually lowers across the summer, dropping to 35 cm or more below the peat surface in summers with particularly low precipitation. Mean cumulative rainfall for the region (1989–2019) for the months of May through August was 386.3 ± 133.1 mm (National Centers for Environmental Information, 2021). Across the same months, cumulative precipitation was 210.1 mm in 2020 and 563.0 mm in 2021 (Table 1). Monthly cumulative precipitation in 2020 and 2021 differed the most from historical trends in July and August. In August of 2020, cumulative precipitation was only 20% of the 30-year average (19.5 mm vs. 99.5 mm), while in July of 2021 cumulative precipitation was > 330% of the 30-year average (330.8 mm vs. 98.3 mm).

The county containing Sallie's Fen experienced moderate to severe drought conditions from early June through the end of the study period in 2020. In 2021, abnormally dry conditions occurred in

Table 1. Monthly Precipitation and Air Temperature in 2020–2021 Compared to 30-Year Average

Period	Cumulative precipitation (mm)			Air temperature (°C)		
	1989–2019*	2020§	2021§	1989–2019*	2020§	2021§
May	94.7 ± 65.4	57.1	94.7	17.06 ± 5.9	20.8 ± 7.1	21.0 ± 4.3
June	100.7 ± 60.6	60.9	37.0	22.3 ± 5.3	25.9 ± 3.6	20.0 ± 3.5
July	98.3 ± 59.5	72.6	330.8	25.3 ± 4.3	28.2 ± 3.7	26.0 ± 4.0
August	99.5 ± 51.3	19.5	100.5	24.9 ± 4.0	26.5 ± 3.4	29.0 ± 3.4
Seasonal	386.8 ± 133.1	210.1	563.0	22.4 ± 5.9	25.3 ± 5.42	23.8 ± 5.22

Values for 1989–2019 cumulative precipitation and all air temperature values are presented as mean ± 1 standard deviation.
**1989–2019 data are from a station in Durham, NH approximately 20 km away from the field site established prior to the Barrington, NH station.*
§Precipitation data for 2020–21 data are from a station in Barrington, NH from NOAA National Centers for Environmental Information. Air temperatures from 2020 to 21 reflect temperatures collected during field flux measurements.

early summer prior to heavy rainfall in July. While both seasons contained dry periods, a larger late-winter snowpack in 2021 (Figure S2) contributed to higher spring water table levels at Sallie's Fen. Considering both precipitation patterns during the study period as well as antecedent conditions, hereafter we refer to the 2020 and 2021 sample seasons as the ''dry'' and ''wet'' sampling years, respectively.

Methane Flux and δ^{13}C–CH_4 Measurements

Static chamber CH_4 flux measurements were conducted weekly to bi-weekly from May through August at 10 collars following the methods described in Carroll and Crill (1997) and Treat and others (2007). The median number of days between flux measurements was 8 days in 2020 and 11 days in 2021. Monthly mean CH_4 fluxes by microform and across all collars are reported in Table S2. Briefly, a clear 0.4 m^3 chamber (aluminum frame covered in Teflon film) was placed into grooved aluminum collars and left open for 5–10 min to minimize potential disturbance and allow air inside the chamber to return to ambient CH_4 concentration. The chamber was equipped with fans to maintain a well-mixed chamber headspace throughout the measurement period.

To measure CH_4 flux, the chamber was closed and covered with a shroud to block out light and minimize changes in temperature during the measurement period. Five 60 ml headspace gas samples were taken every 2 min over a 10 min period using polypropylene syringes equipped with three-way stopcocks. Headspace gas samples were injected into pre-evacuated 30 ml serum vials equipped with silicon septa and a crimp top in the field for storage until laboratory analysis.

Mixing ratios of CH_4 in the chamber headspace sample were determined via analysis with a gas chromatograph equipped with a flame ionization detector (GC-FID, Shimadzu GC-14A). The GC-FID was operated with detector and injector temperatures of 130, 50 °C column temperature, and an ultra-high purity nitrogen (UHP N_2) carrier gas flow rate of 30 mL min^{-1} through a 2 m 1/8-inch o.d. stainless steel packed column (HayeSepQ 100/120). The GC-FID was calibrated using standards of 2.006 ppm CH_4. The 2.006 ppm standard was a breathing air cylinder calibrated against standards from NOAA's Earth System Research Laboratory's Global Monitoring Division's Carbon Cycle Greenhouse Gases Group. The standard error of 10 standard injections on any analysis day was ≤ 0.1%. Each sample was run twice, and the average CH_4 concentration was used for the final flux calculations. Methane fluxes were calculated as the slope of the linear regression of CH_4 concentration over the 10 min measurement period using the following equation:

$$\text{mg CH}_4\text{m}^{-2}\ \text{d}^{-1} = \Delta * \frac{P}{R*T} * \frac{V_c}{A_c} * \frac{1440\ \text{min}}{d} * \frac{16\text{mol CH}_4}{1\text{g}} * \frac{1\ \text{mg}}{1000\ \mu\text{g}} \quad (1)$$

where Δ is the change in CH_4 concentration (in ppm or µmol/mol) per minute, P is pressure in atm, R is the ideal gas constant (in m^3 atm mol^{-1} K^{-1}), T is air temperature during the flux measurement in K, V_c and A_c are the chamber volume (in m^3) and area (in m^2). Flux measurements were quality filtered following Treat and others (2007) and Noyce and others (2014) to include only fluxes with sufficient linear fits; fluxes were rejected if they did not fit the 95% confidence interval with respect to the coefficient of determination: $n = 3$ ($r^2 = 0.95$), $n = 4$ ($r^2 = 0.87$), and $n = 5$ ($r^2 = 0.75$). Quality filtering excluded measurements with starting CH_4 mixing ratios substantially above ambient, indicating that the disturbance from chamber placement affected the resulting flux measurement. The quality filtering protocol effectively removed all negative flux measurements (n = 12 of 228 total flux observations) as they were either nonlinear or due to improper chamber placement. Approximately 20% of the CH_4 flux measurements were discarded during quality filtering, but the mean (174.4 vs. 174.7 mg CH_4 m^{-2} d^{-1}) and median (84.5 vs. 84.7 mg CH_4 m^{-2} d^{-1}) of the total (n = 228) and quality filtered (n = 181) flux datasets were not significantly different. Methane flux values were log transformed prior to statistical analysis.

Samples for isotopic analysis of CH_4 emissions were collected twice monthly at the time of CH_4 flux measurements. The median number of days between flux isotope sample collection was 14 days in 2020 and 15 days in 2021. Monthly mean $\delta^{13}C$–CH_4 by microform and across all collars are reported in Table S2. Seven 60 ml gas samples (420 ml total) were collected in polypropylene syringes equipped with three-way stopcocks before the chamber lid was closed (T_0) and after the chamber had been closed for an additional 30 min after the end of the CH_4 flux measurement (T_f). This sampling scheme allowed for accumulation of sufficient chamber headspace CH_4 for calculation of isotope source signatures according to the change in CH_4 mole fraction and isotope composition over the measurement period. Ambient and chamber headspace gas samples were injected into pre-evacuated 200 ml serum vials equipped with butyl rubber septa and a crimp top in the field for storage until laboratory analysis.

The $\delta^{13}C$–CH_4 values of the chamber samples were measured using an Aerodyne dual Tunable Infrared Laser Direct Absorption Spectroscopy (TILDAS) analyzer at UNH described in Perryman and others (2022). The TILDAS was configured with an automated sampling system to measure both high concentration samples via direct injection and samples with CH_4 concentrations close to ambient levels from attached flasks. The isotopic composition of the standards tanks was determined using an Aerodyne calibration system. The spectroscopic isotope ratios of 4 Isometric (now Airgas) CH_4 isotope standards were measured at diluted concentrations ranging from < 1 to 12 ppm. A Keeling plot analysis was used to determine the relationship between the spectroscopic and standard isotope ratios of the Isometric standards. The linear relationship was then applied to the corresponding measured spectroscopic isotopic ratios of the UNH calibration tanks. The instrument precision was 0.1‰ for $\delta^{13}C$–CH_4. Aliquots of the T_0 and T_F chamber samples were also analyzed for CH_4 mole fraction on the GC–FID as described above.

We used Keeling plot analysis to determine the $\delta^{13}C$–CH_4 source signature for CH_4 fluxes. The $\delta^{13}C$–CH_4 value of each sample is plotted against the reciprocal mole fraction of CH_4 ($1/CH_4$), and the resulting y-intercept represents the isotopic signature of the CH_4 source (Keeling 1958; Pataki and others 2003). The isotope source signature from each chamber measurement was calculated following Fisher and others (2017) if there was at least a 0.05 ppm CH_4 increase in the chamber during the 40 min it was closed:

$$\delta^{13}C = (\delta^{13}C_{Tf}C_{Tf} - (\delta^{13}C_{T0}C_{T0})/(C_{Tf} - C_{T0}) \quad (2)$$

in which C_{T0} and C_{Tf} are the CH_4 mole fraction (determined via GC-FID) and ${}^{13}C_{T0}$ and ${}^{13}C_{Tf}$ are the isotope composition of the respective chamber samples.

Climatological Variables

Flux measurements were coupled with simultaneous measurements of peat surface temperature, 10 cm peat temperature, and ambient air temperature. Water table depth was also measured at the time of CH_4 flux measurements using PVC wells installed adjacent (< 50 cm) to the flux collars. Water table depth was calculated as the difference between the distance from top of the PVC well to the water table position and the distance from top of the PVC well to the peat surface, multiplied by −1 so that values for water table depth below the peat surface are < 0 and values for water table depth above the peat surface are > 0. Precipitation data from a weather station in Barrington, NH retrieved from the NOAA National Centers for Environmental Information (https://www.climate.gov/maps-data/dataset/past-weather-zip-code-data-table) was used to calculate cumulative precipitation between flux and/or $\delta^{13}C$–CH_4 measurements, as well as the number of days between flux and/or $\delta^{13}C$–CH_4 measurements and the last rain event.

Data Analysis and Visualization

Statistical analysis and data visualization were performed in *R* v4.0.3. The level of significance for all analyses was 0.05. Data preparation was conducted using the *dplyr* (Wickham and others 2021) and *lubridate* (Grolemund and Wickham 2011) packages. Data and analyses were visualized using *ggplot2* (Wickham, 2016) and *patchwork* (Pedersen 2020) packages. All mixed effects models described below were constructed using the *nlme* package (Pinheiro and others 2021). Collar ID was included as a random effect in all models to account for repeated measures. We used ANOVA to assess the significance of fixed effects and their interactions. Post hoc Tukey tests via the *emmeans* package (Lenth 2021) were performed for pairwise comparisons. Methane fluxes were $\log_{10}$-transformed prior to statistical analysis.

We assessed the effect of microform, sampling months, sampling years, and the interaction of month and year on water table depth and air/peat temperatures using mixed effects models of the form:

$$\text{Temperature or Water Table Depth} = f(\text{microform} + \text{month} * \text{year} + 1|\text{collar ID}) \quad (3)$$

We assessed the impact of microform, month, sampling year, and their interactions (hereafter, spatiotemporal variation) on CH_4 fluxes and flux $\delta^{13}C$–CH_4 using mixed effects models of the form:

$$CH_4\text{flux or Flux } \delta^{13}C - CH_4 = f(\text{microform} * \text{month} * \text{year} + 1|\text{collar ID}) \quad (4)$$

Finally, we used linear mixed effects models to assess relationships between CH_4 fluxes and $\delta^{13}C$–CH_4 and climatological variables. We analyzed data from the dry (2020) year and wet (2021) year separately to assess if significant drivers of CH_4 emissions differed between the two years. These linear mixed effects models were of the form:

$$CH_4\text{ flux or } \delta^{13}C - CH_4 = f(\text{climatological variable} + 1|\text{collar ID}) \quad (5)$$

in which climatological variables included water table depth, weekly cumulative precipitation prior to the measurement date, the number of days between the measurement date and the last rain event, peat temperature at both the peat surface and 10 cm, and air temperature.

We determined the amount of variance explained by just the fixed effect (marginal, R^2_m) and together with the random effect (conditional, R^2_c) using the *MuMIn* package (Bartoń 2020). In the main manuscript text and figures we report R^2_m.

Results

Seasonal Water Table Depth and Temperature

Water table depth exhibited large spatiotemporal variation and was influenced by the timing and amount of precipitation across both summers (Figure 1). Water table depth was significantly different between microforms ($p = 0.035$) and years ($p < 0.0001$; Table S3). Across all collars the water table was significantly lower in 2020 (−20.8 ± 11.5 cm) than 2021 (−4.5 ± 7.1 cm), reflecting the lower precipitation in summer 2020 (Table 1). Across both sampling years, the water table was lower in hummocks than wet microforms ($p = 0.0273$). Seasonal average water table depth for hummock, lawn, and wet collars in 2020 were −30.1 ± 15.6 cm, −26.0 ± 14.7 cm, and −20.7 ± 11.9 cm, respectively, and −7.9 ± 5.1 cm, −6.1 ± 5.1 cm, and 2.3 ± 7.1 cm in 2021. The seasonal pattern in water table depth also varied between the two years ($p < 0.001$, Table S3). Under drought conditions in 2020 water table depth significantly decreased from May to June ($p < 0.0001$) and July to August ($p < 0.0001$), while in 2021 water table depth was significantly lower in June than any other month, as flooding after rainstorms in July raised the water table depth to levels comparable to those in May (Figure 1, Table S4).

Surface temperature, peat temperature (at 10 cm depth), and air temperature did not vary between microforms (Table S3). Peat surface and air temperature during flux measurements were higher in 2020 than 2021, ($p = 0.0017$ and $p = 0.04$, respectively), while peat temperature at 10 cm was not significantly different between years. In 2020 mean peat surface and air temperature during flux measurements were 2.2 and 1.5 °C warmer than 2021, respectively. Peat and air temperature also varied seasonally. Across both years peat temperature at 10 cm increased from late spring to mid-summer (Figure 1, Table S3). In 2020 peat temperature increased significantly from May to June to July ($p < 0.05$ for all), while in 2021 peat temperature was lower in May than June through August, during which peat temperature did not vary significantly (Table S4). Peat surface temperature was highest in July in both years, but overall peat surface temperature varied less across months in 2021 than in 2020. Air temperature increased from the beginning of sampling in the spring to mid-summer of both years, but in 2020 air temperature was significantly lower in May than June–

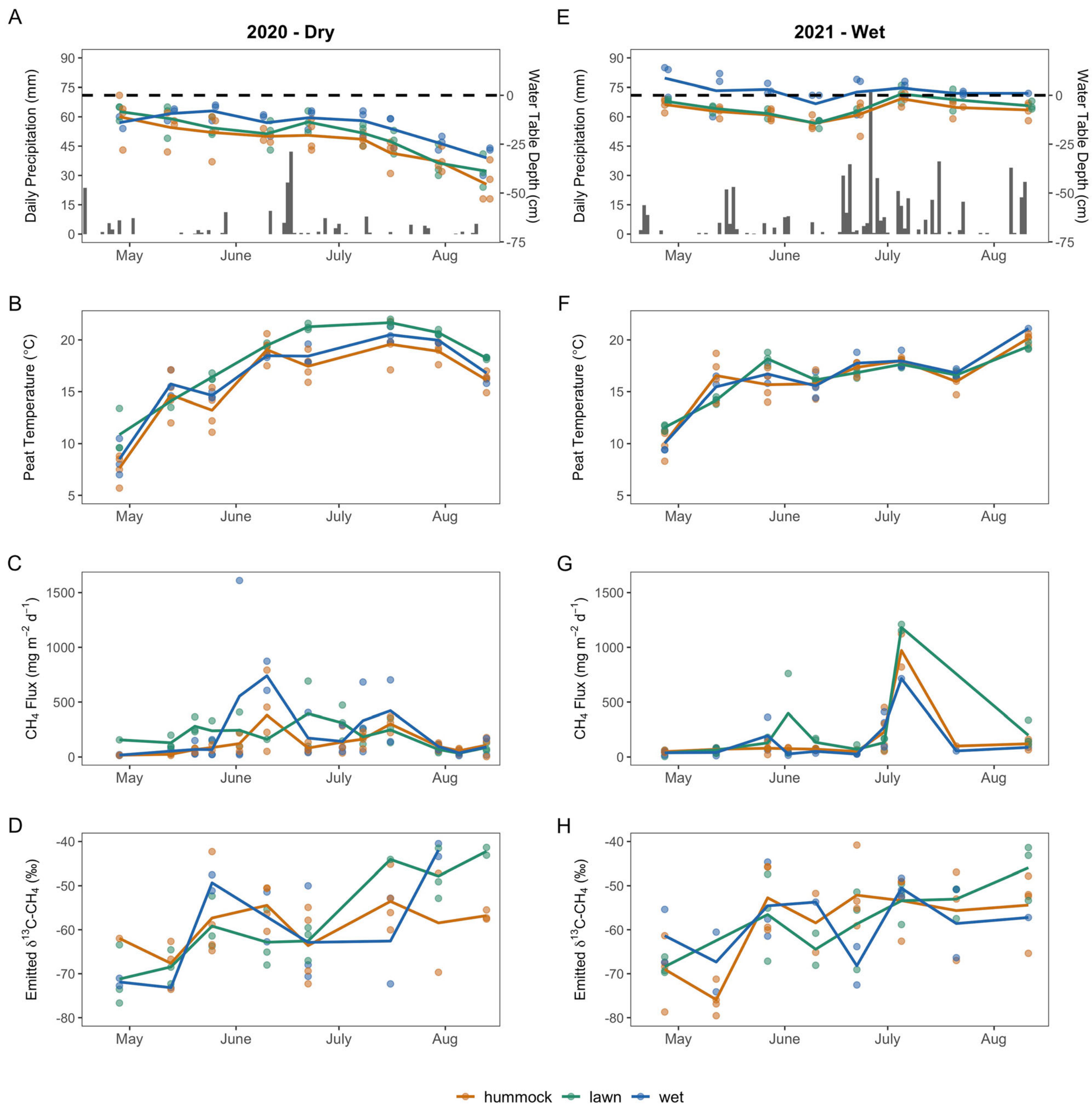

Figure 1. Daily precipitation (in mm, data from NOAA NCEI) and water table depth (in cm; A, E), peat temperature at 10 cm (°C; B, F), CH_4 fluxes (in mg CH_4 m^{-2} d^{-1}; C, G), and the isotopic composition ($\delta^{13}C$–CH_4) of CH_4 fluxes (in ‰; D, H) across the study period in 2020 (**A**–**D**) and 2021 (**E**–**H**). Points for water table depth, peat temperature, CH_4 fluxes, and $\delta^{13}C$–CH_4 are individual measurements, with lines representing running means of each collar type. Orange, green, and blue points and lines represent hummock, lawn, and wet collars; respectively. For panels A and E, the dashed black line represents the ground surface, with negative water table depth values indicating a water table position below the ground surface.

August, whereas in 2021 air temperature was similar in May and June but higher in July and August (Table 1, Table S4).

Spatiotemporal Variation in CH_4 Fluxes and $\delta^{13}C$–CH_4

Methane emissions were highly variable, with fluxes ranging from 3.1 to 1610.8 mg CH_4 m^{-2} d^{-1} (n = 181, Figure 1) and $\delta^{13}C$–CH_4 from −79.6 to −

40.5‰ (n = 125, Figure 1) across the study period. Methane fluxes nor $\delta^{13}C–CH_4$ were not significantly different between microforms (Figure 2A–B; Table S5). Mean seasonal CH_4 fluxes for hummocks, lawns, and wet collars in the dry year were 140.9 ± 150.3, 202.5 ± 145.8, and 207.7 ± 334.7 mg CH_4 m^{-2} d^{-1}, respectively, while in the wet year they were 151.1 ± 233.5, 222.1 ± 331.7, and 125.5 ± 173.8 mg CH_4 m^{-2} d^{-1} (Table S2). Mean seasonal $\delta^{13}C–CH_4$ values from hummocks, lawns, and wet collars in the dry year were −58.7 ± 8.1, −59.3 ± 10.2, and −59.1 ± 12.1‰, respectively, while in the wet year they were −59.1 ± 10.1‰, −56.8 ± 8.9‰, and −58.6 ± 8.6‰ (Table S2). The seasonal pattern of $\delta^{13}C–CH_4$ varied between microforms (p = 0.03; Figure S3B, Table S6). Emitted $\delta^{13}C–CH_4$ increased across the growing season in laws, while in hummocks $\delta^{13}C–CH_4$ remained stable June through August after an initial increase from May to June. At the seasonal scale, neither CH_4 emissions nor $\delta^{13}C–CH_4$ varied between the dry and wet year (p > 0.05 for both). Across Sallie's Fen, seasonal average CH_4 fluxes were 181.5 ± 227.3 mg CH_4 m^{-2} d^{-1} in the dry year (n = 103) and 165.8 ± 254.2 mg CH_4 m^{-2} d^{-1} in the wet year (n = 78). Mean seasonal $\delta^{13}C–CH_4$ was −59.0 ± 9.9‰ in the dry year (n = 60) and −58.3 ± 9.7‰ in the wet year (n = 65).

Methane emissions varied strongly between months in both years (p < 0.001; Figure 3). Across both years CH_4 fluxes were lowest in May

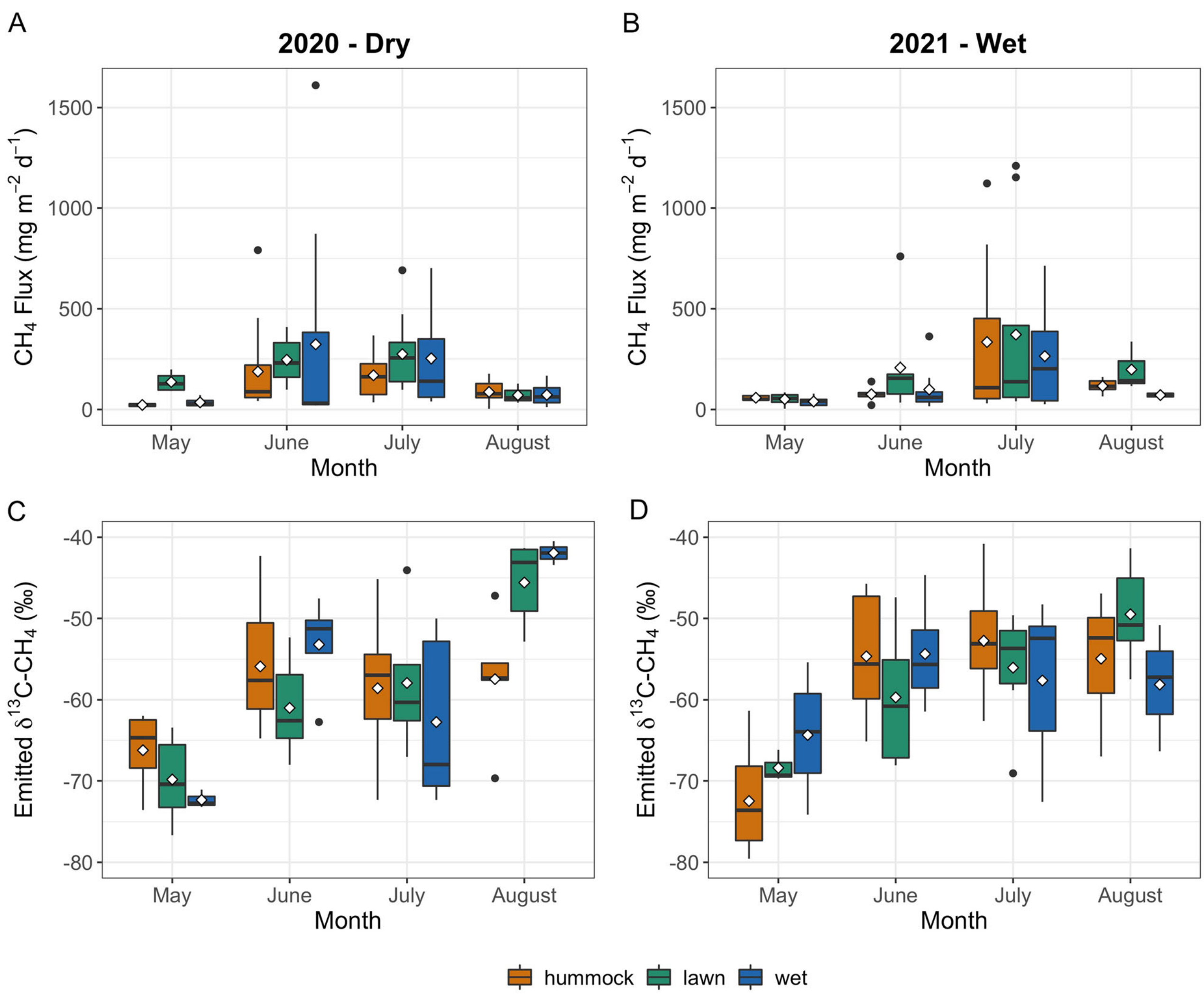

Figure 2. Methane fluxes (**A**, **B**; n = 181) and the isotopic composition ($\delta^{13}C–CH_4$) of CH_4 fluxes (**C**, **D**; n = 125) across the 2020 (A, C) and 2021 (B, D) study period by month and collar type. White diamonds represent the mean CH_4 flux and $\delta^{13}C–CH_4$ values and black lines represent median values. Boxes represent 25th and 75th percentiles. Orange, green, and blue boxes represent hummock, lawn, and wet collars; respectively.

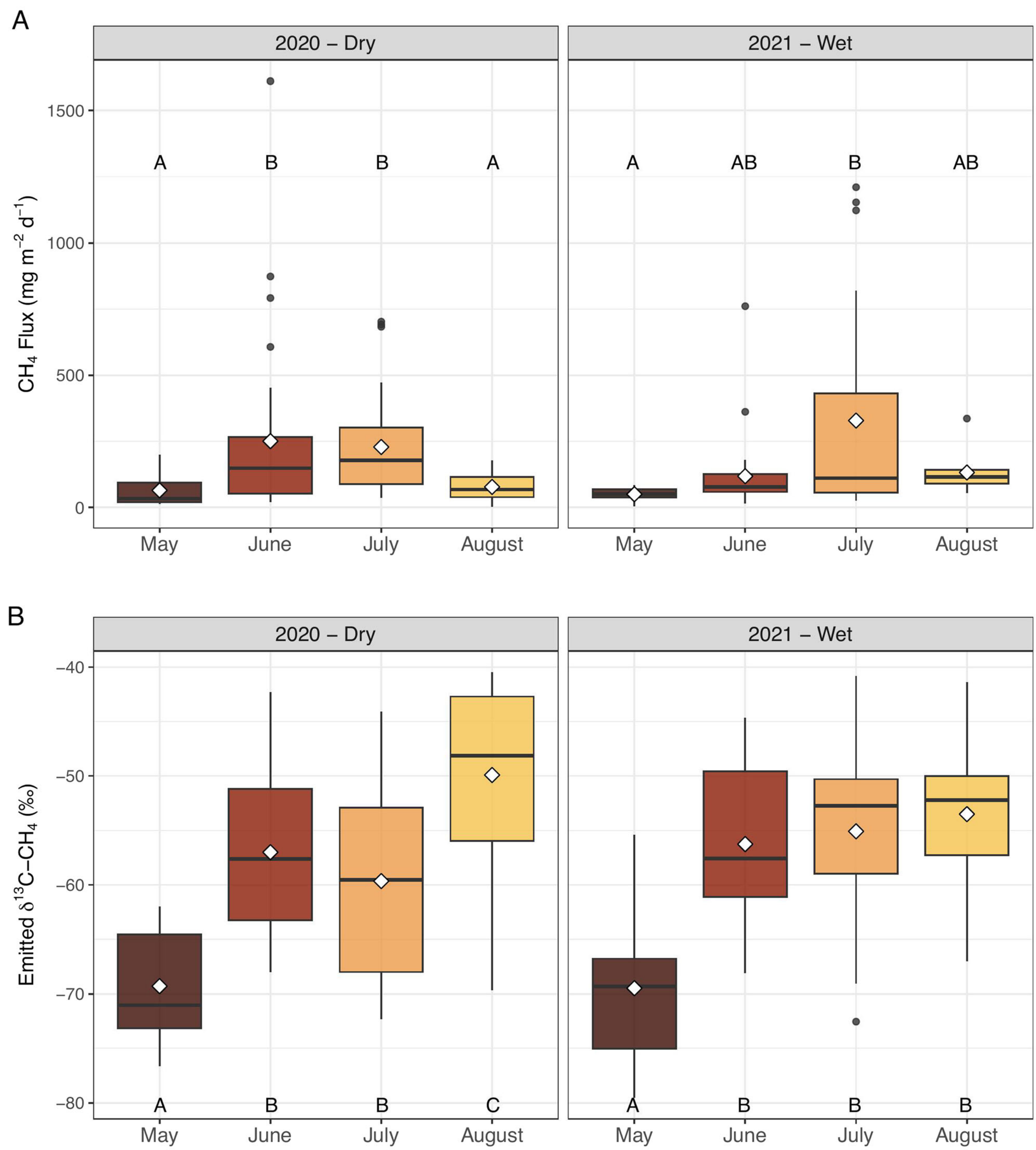

Figure 3. Methane fluxes (A, n = 181) and the isotopic composition ($\delta^{13}C–CH_4$) of CH_4 fluxes (B, n = 125) across 2020 and 2021 study period by month. White diamonds represent the mean CH_4 flux and $\delta^{13}C–CH_4$ values and black lines represent median values. Boxes represent 25th and 75th percentiles. Capital letters represent significant differences between months within each year.

(65.0 ± 61.32 and 50.3 ± 23.9 mg CH_4 m^{-2} d^{-1}, respectively) and highest in July (228.9 ± 183.9 and 328.9 ± 394.3 mg CH_4 m^{-2} d^{-1}, respectively) and $\delta^{13}C–CH_4$ was lowest in May (−69.3 ± 7.2.0 and −69.5 ± 6.9‰, respectively) and highest in August (−49.9 ± 8.9 and −53.5 ± 7.6‰, respectively). The interaction term between month and year was not significant in either of the mixed effects models for CH_4 fluxes nor $\delta^{13}C–CH_4$ (Table S5). Indeed, neither CH_4 fluxes nor $\delta^{13}C–CH_4$ varied between years within any month ($p > 0.05$ for all pairwise comparisons). However, whether CH_4 fluxes and $\delta^{13}C–CH_4$ were significantly different between months did depend on the year (Figure 3; Table S7-8). In the dry year, CH_4 fluxes increased between May and June ($65.0 \pm 61.3–251.0 \pm 329.7$ mg CH_4 m^{-2} d^{-1}; $p = 0.0031$) and then decreased from July to August ($228.9 \pm 183.9–77.8 \pm 49.2$ mg CH_4 m^{-2} d^{-1}; $p = 0.0003$), while in the wet year CH_4 fluxes were only significantly different between May and July (50.3 ± 23.9 vs. 328.9 ± 394.3 mg CH_4 m^{-2} d^{-1}; $p = 0.0001$). Likewise, while $\delta^{13}C–CH_4$ increased ~ 10‰ from May to June in both years, $\delta^{13}C–CH_4$ increased significantly from July to August (-59.7 ± 9.1 to -49.9 ± 8.9‰, $p = 0.0014$) in the dry year, but there was no significant change in $\delta^{13}C–CH_4$ from June through August of the wet year (Figure 3, Table S8).

Effect of Climatological Variables on CH_4 Fluxes and $\delta^{13}C–CH_4$

We did not observe a significant effect of water table depth (Figure 4) nor the number of days since the last rain event (Table S9) on CH_4 fluxes in either year. In the wet year, CH_4 emissions increased with increasing weekly cumulative precipitation ($p = 0.0022$, $R^2{}_m = 0.12$, Figure 4D), but there was no relationship between weekly cumulative precipitation and CH_4 emissions in the dry year. Methane emissions increased with peat temperature at 10 cm in both years ($p < 0.001$, $R^2{}_m = 0.13$ and $p < 0.001$, $R^2{}_m = 0.16$, Figure 4), but surface peat temperature ($p < 0.001$) and air temperature ($p = 0.018$) only had a significant effect on CH_4 fluxes in the dry year (Figure 4, Table S9).

Under drought conditions in 2020, $\delta^{13}C–CH_4$ increased as water table levels dropped ($p = 0.008$, $R^2{}_m = 0.12$), but water table depth did not have a significant effect on $\delta^{13}C–CH_4$ in the wet year (Figure 5A–B). By contrast, in the wet year $\delta^{13}C–CH_4$ increased with increasing weekly cumulative precipitation ($p = 0.0018$, $R^2{}_m = 0.15$, Figure 5D) but there was not a significant effect of weekly cumulative precipitation on $\delta^{13}C–CH_4$ in the dry year. Like CH_4 emissions, $\delta^{13}C–CH_4$ increased with peat temperature at 10 cm in both years ($p < 0.001$, $R^2{}_m = 0.19$ and $p < 0.001$, $R^2{}_m = 0.17$, Figure 5E–F). Emitted $\delta^{13}C–CH_4$ also increased with increasing air temperature in both years (Table S9, Figure 5G–H).

Figure 4. Effect of year and **A**, **B** water table depth, **C**, **D** ▶ cumulative weekly precipitation, **E**, **F** peat temperature at 10 cm and **G**, **H** air temperature on CH_4 emissions. Figure panels in the left column with red diamond points show data from 2020 and figure panels in the right column with blue circular points show data from 2021. Note the different x-axis scales for water table depth in panels A and B. Shaded regions represent the 95% confidence interval associated with each linear relationship. Panels without trend lines reflect fixed effects that did not have a significant effect on CH_4 emissions.

Discussion

Limited Differences in CH_4 Emissions Across Microforms

Significant differences in CH_4 emissions between microforms with varying water table depth and vegetation have been observed across northern and temperate peatlands (for example Bubier and others 1993; Bubier and others 1995; Frenzel and Karofeld 2000). However, we observed similar seasonal average CH_4 fluxes across the hummock, lawn, and wet collars despite differences in water table position (Figure 1) and vegetation communities (Figure S1). In the dry year the collar with the highest seasonal mean water table also had the largest seasonal mean CH_4 flux (Table S5), as was observed in a previous study that synthesized 5 years of CH_4 flux measurements from Sallie's Fen (Treat and others 2007). However, in the wet year the highest mean seasonal CH_4 flux was not observed from the collar with the highest mean seasonal water table. One possible explanation for the lack of variability in CH_4 fluxes across microforms is that large seasonal variability in water table depth (−53 to 0 cm in 2020; −23 to 14 cm in 2021) outweighed the impact of plot-scale variability in water table levels on CH_4 emissions. Secondly, the ratio of methanogenic to methanotrophic microbial taxa in the surface peat (~ 5–15 cm depth) has been found to be a strong control of CH_4 fluxes (Rey-Sanchez and others 2019) in temperate peatlands. Previous work at Sallie's Fen found that the ratio of methanotrophs to methanogens at 10 cm was higher in hummocks where the water table was > 10 cm below the peat surface than in lawns where the water table was < 10 cm (Perryman and others 2022). In this study, seasonal average water table depth was > 10 cm below the peat surface in the dry year and < 10 cm below the peat surface in the wet year across microforms. As such, the microbial community composition in

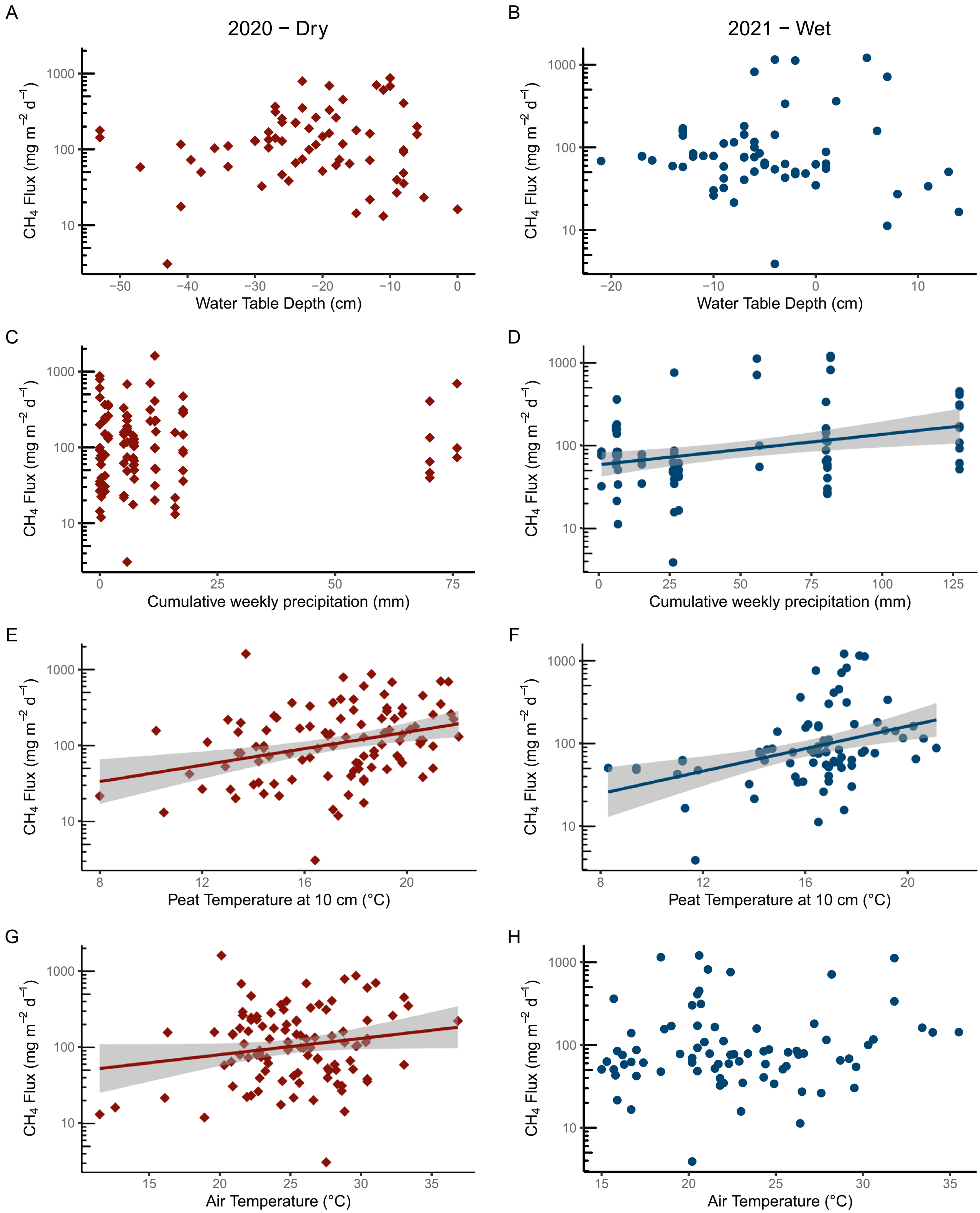
A
2020 − Dry
B
2021 − Wet
CH4 Flux (mg m-2 d-1)
Water Table Depth (cm)
C
D
Cumulative weekly precipitation (mm)
E
F
Peat Temperature at 10 cm (°C)
G
H
Air Temperature (°C)

the surface peat may have been more similar across microforms during this study than in past observations, potentially weakening the effect of microbial community composition on CH_4 fluxes and lessening the spatial variability in CH_4 emissions.

While it is well-established that $\delta^{13}C–CH_4$ varies between northern peatland types with variable hydrology, plant-cover, and nutrient status (for example, Chasar and others 2000; Hornibrook and Bowes 2007), there are fewer measurements explicitly considering the impact of microtopography on $\delta^{13}C–CH_4$. We did not observe significant differences in $\delta^{13}C–CH_4$ between microforms, consistent with previous manual measurements from a Finish boreal peatland (Dorodnikov and others 2013). Recent work from a Swedish hemiboreal mire with similar differences in elevation between microforms as at Sallie's Fen ($\leq$ 20 cm) observed large (5–15‰) microtopographic variation in CH_4 fluxes and $\delta^{13}C–CH_4$ using an automated chamber system (Rinne and others 2022). Spatial differences in $\delta^{13}C–CH_4$ at the Swedish mire were likely due to variation in methanogenic pathways in accordance with aboveground vegetation, as the largest $\delta^{13}C–CH_4$ values were observed from areas dominated by aerenchymatous sedges (Rinne and others 2022) which promote acetoclastic methanogenesis and therefore larger $\delta^{13}C–CH_4$ values via root exudation of labile substrates (Heffernan and others 2022; Hodgkins and others 2014). We did not observe larger $\delta^{13}C–CH_4$ values from lawns with more abundant sedges (Figure S1; Figure S3), suggesting spatial differences in methanogenic pathways were small. This is consistent with earlier observations from Sallie's Fen which found that the community composition of methanogens did not vary across microtopography (Perryman and others 2022). Furthermore, our measurements do not suggest that the larger abundance of sedges in lawns (Figure S1) promoted CH_4 emissions via plant-mediated transport. The lawns did not have significantly higher CH_4 emissions nor lower $\delta^{13}C–CH_4$ (Figure S3, Table S1) as would be expected if plant-mediated transport was a dominant emissions pathway from these collars (Chanton 2005). As sedges were present in at least low proportions in all microforms in our study, their influence on CH_4 production and emissions across microforms was likely less pronounced than previous work comparing sites where sedges were absent (Greenup and others 2000) or experimentally removed (Noyce and others 2014; Waddington and others 1996) to sites dominated by sedges.

CH_4 Emissions from Dry and Wet Years

We did not observe significant differences in CH_4 fluxes and $\delta^{13}C–CH_4$ between the dry and wet years, despite significant differences in water table dynamics and precipitation between years (Figure 1). Mean seasonal CH_4 fluxes in 2020 and 2021 of 181.5 ± 227.3 and 165.8 ± 254.2 mg CH_4 m^{-2} d^{-1}, respectively, are of similar magnitude and variability as recent observations from Sallie's Fen (Noyce and others 2014; Treat and others 2007) as well as measurements across other temperate peatlands (Turetsky and others 2014). Our results contrast prior work assessing the impact of low and high precipitation years on CH_4 emissions from northern peatlands. Across peatland sites, drought and/or drainage has been observed to reduce CH_4 fluxes (for example, Kettunen and others 1999; Knorr and others 2008b; Strack and others 2004). Conversely, wet years are often associated with elevated CH_4 emissions. For example, Bubier and others (2005) observed that CH_4 fluxes from boreal peatlands were 60% higher in a year that received 40% more precipitation. While cumulative May to August precipitation in 2021 was 168% higher than in 2020 at our study site, and water table depth was consistently higher as well, we did not observe higher CH_4 emissions in 2021.

High CH_4 fluxes during years with lower water table level have been observed previously at Sallie's Fen (Carroll and Crill 1997; Treat and others 2007). Potential mechanisms sustaining CH_4 emissions despite low water table levels include both high CH_4 production during warm periods and possible episodic degassing of stored CH_4 as water table levels drop. While peat temperature was not significantly different between the dry and wet years (Table S3), high peat temperatures in July–August of the dry year (Figure 1) may have sustained high rates of CH_4 production at depth even as the water level dropped (Dunfield and others 1993; Kolton and others 2019). Depressurization-driven degassing of stored CH_4 has been observed across northern peatland sites (Glaser and others 2004; Strack and others 2005), including at Sallie's Fen where Goodrich and others (2011) observed that peak ebullition corresponded with decreasing water table depth and high peat temperatures. While our quality control methods for CH_4 flux calculations would exclude large episodic releases that resulted in nonlinear trends in chamber headspace CH_4 accumulation, they could capture steady low-levels of ebullition. It has been suggested that CH_4 transported by ebullition may be

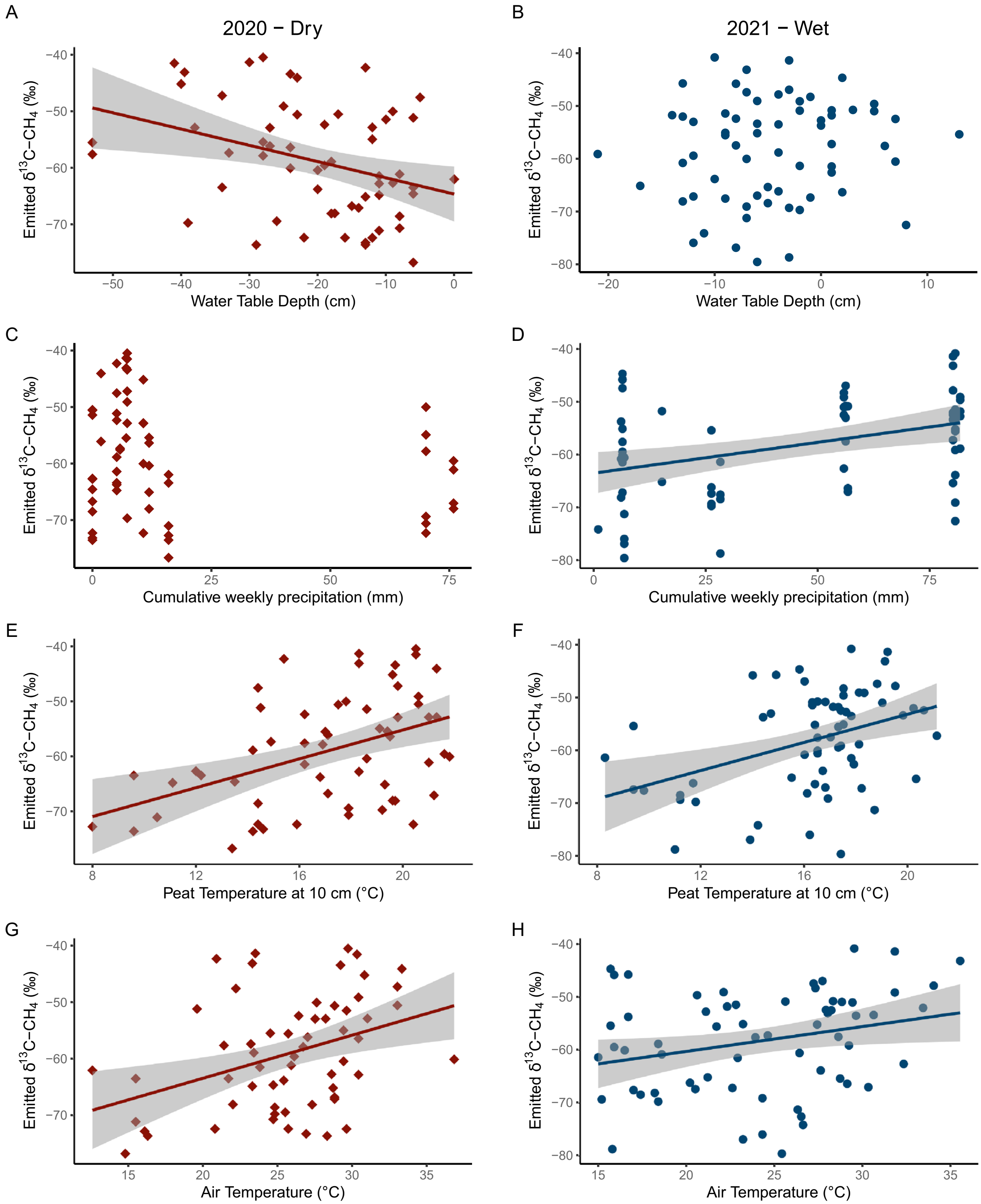

Figure 5. Effect of year and **A**, **B** water table depth, **C**, **D** cumulative weekly precipitation, **E**, **F** peat temperature at 10 cm and **G**, **H** air temperature on emitted $\delta^{13}C–CH_4$. Figure panels in the left column with red diamond points show data from 2020 and figure panels in the right column with blue circular points show data from 2021. Note the different x-axis scales for water table depth in panels A and B. Shaded regions represent the 95% confidence interval associated with each linear relationship. Panels without trend lines reflect fixed effects that did not have a significant effect on emitted $\delta^{13}C–CH_4$.

relatively ^{13}C depleted, assuming the CH_4 is transported from an anoxic depth and bypasses ^{13}C-enriching zones of CH_4 oxidation (Chanton 2005). However, using both automated (Santoni and others 2012) and manual (Roddy 2014) ebullition measurements, prior work has determined that ebullition emits CH_4 with a mean $\delta^{13}C$–CH_4 value of approximately −57 to −54‰ at Sallie's Fen, values which are comparable to those we observed from June–August of both years (Figure 2, Table S2). As such, our $\delta^{13}C$–CH_4 measurements cannot resolve if ebullitive emissions may explain why CH_4 fluxes were not lower in the dry year.

We hypothesized that $\delta^{13}C$–CH_4 would be higher under dry conditions in 2020 which can promote CH_4 oxidation (Moore and Dalva 1993; White and others 2008) and therefore increase $\delta^{13}C$–CH_4 (Coleman and others 1981; Whiticar 1999). However, we did not observe a significant difference in $\delta^{13}C$–CH_4 between the dry and wet year at the seasonal timescale. Mean seasonal $\delta^{13}C$–CH_4 was −59.0 ± 9.9‰ in 2020 and −58.3 ± 9.7‰ in 2021. Seasonal average $\delta^{13}C$–CH_4 at Sallie's Fen was comparable to that observed from a raised bog in the Glacial Lake Agassiz Peatland Complex (−58.7 ± 5.8‰) with similar seasonal water table position to Sallie's Fen, but higher than from a fen (−63.6 ± 1.4‰) in which the water table was above the ground surface from June to September (Chasar and others 2000). The seasonal average $\delta^{13}C$–CH_4 from both years was also in better agreement with observations from a dry period (~ 56‰) in a *Carex spp.* dominated rich fen in Alberta than the seasonal average under normal flooded conditions (~ −64 to −66‰, Popp and others 1999), likely because the normal water table levels at the Alberta site were higher than observed at Sallie's Fen even in the wet year.

Drivers of Seasonal Variation in CH_4 Emissions in Dry and Wet Years

Monthly variation in CH_4 flux and $\delta^{13}C$–CH_4 was larger than interannual variation or variation between microforms. Like in past studies at Sallie's Fen, CH_4 emissions increased from May to July (Carroll and Crill 1997; Noyce and others 2014; Treat and others 2007), and in both years $\delta^{13}C$–CH_4 was higher at the end of the summer than the beginning (Figure 3). Increasing peat temperatures early in the summer likely increased CH_4 production rates and therefore CH_4 emissions, given the strong relationship we observed between peat temperature and CH_4 fluxes in both years (Figure 4). Increased plant productivity likely also contributed to the large increase in CH_4 emissions from May to July (Bellisario and others 1999; Joabsson and others 1999; Whiting and Chanton 1993), as both net ecosystem exchange and photosynthesis increase steadily from the beginning of the growing season to their peak values midsummer at Sallie's Fen (Carroll and Crill 1997; Treat and others 2007). The shift towards higher $\delta^{13}C$–CH_4 we observed across both summers is consistent with prior work indicating that acetoclastic methanogenesis becomes more dominant across the growing season (Avery and others 1999; Keller and Bridgham 2007; Kelly and others 1992). Acetoclastic methanogenic archaea may become more abundant as temperature and substrate availability increase (Chang and others 2020; Wilson and others 2021), increasing total CH_4 production as well as the influence of acetoclastic methanogenesis on emitted $\delta^{13}C$–CH_4. We observed that $\delta^{13}C$–CH_4 increased with air and peat temperature both years (Figure 5), suggesting that warmer temperatures promoted a shift towards acetoclastic methanogenesis.

In both years mean $\delta^{13}C$–CH_4 increased from July to August as mean CH_4 fluxes decreased (Table S2); however, changes in CH_4 emissions and $\delta^{13}C$–CH_4 from July to August were only significant in the dry year (Table S7-8). In the dry year emissions significantly decreased ($p = 0.0003$; Table S7, Figure 3) and $\delta^{13}C$–CH_4 increased by 10‰ ($p = 0.0014$; Table S8, Figure 3) as the water table depth dropped by > 15 cm. This observation is consistent with previous mesocosm experiments which found that a water level difference of 20 cm between fen mesocosms resulted in a difference of ~ 15‰ in emitted $\delta^{13}C$–CH_4 (White and others 2008) and that lowering water table depth increases dissolved $\delta^{13}C$–CH_4 by ~ 10‰ (Knorr and others 2008a). The paired decrease in CH_4 emissions and increase in $\delta^{13}C$–CH_4 in the dry year suggests that increased CH_4 oxidation, rather than decreased CH_4 production, suppressed CH_4 fluxes in late summer, as CH_4 oxidation increases $\delta^{13}C$–CH_4 (Coleman and others 1981; Whiticar 1999). Furthermore, $\delta^{13}C$–CH_4 increased as the water table depth dropped in the dry year (Figure 5, $p = 0.008$), indicating that the falling water table observed across the dry year increasingly promoted conditions favorable for aerobic methanotrophy (Sundh and others 1994; Yrjälä and others 2011). Kelly and others (1992) also observed a seasonal trend towards higher $\delta^{13}C$–CH_4 that correlated with deeper water table depth in a bog in northern Minnesota and likewise suggest the seasonal pattern they observed in CH_4 emissions was controlled by microbial oxidation.

In the wet year neither CH_4 emissions nor $\delta^{13}C$–CH_4 changed significantly between July and August (Table S7-8). The apparent decrease in CH_4 emissions between July and August of the wet year (Figure 3) was likely due to rainstorms that promoted site flooding and large (> 1000 mg CH_4 m^{-2} d^{-1}) CH_4 fluxes in late July (Figure 1). Our observations are consistent with prior work from temperate peatlands showing that rainstorms substantially increase CH_4 emissions by increasing inundation (Huth and others 2013, 2018). Previously, Frolking and Crill (1994) suggested that heavy rain may suppress CH_4 emissions from Sallie's Fen, but their study included Hurricane Bob in August 1991 which delivered nearly 200 mm of rain in a single day, whereas maximum daily rainfall during our study period in 2021 was 72.6 mm. Furthermore, CH_4 fluxes in August of the wet year (132.4 ± 79.4 mg CH_4 m^{-2} d^{-1}) were similar to previously published growing season CH_4 fluxes of 200–400 mg CH_4 m^{-2} d^{-1} from 2000 to 2004 (Treat and others 2007) and 130–180 mg CH_4 m^{-2} d^{-1} from 2008 to 2011 (Noyce and others 2014), while CH_4 emissions in August of the dry year were lower than historical observations (77.8 ± 49.2 mg CH_4 m^{-2} d^{-1}). Overall, the larger and more significant change in $\delta^{13}C$–CH_4 between July and August of the dry year indicate CH_4 oxidation reduced CH_4 emissions under drought conditions, whereas smaller changes in CH_4 emissions in late summer in the wet year were reflective of episodically large fluxes in July.

Interestingly, the increase in CH_4 emissions after heavy rain in July of the wet year was not associated with a decrease in $\delta^{13}C$–CH_4, as may be expected if rising water table levels suppressed CH_4 oxidation. We did observe that emitted $\delta^{13}C$–CH_4 increased with weekly cumulative precipitation in the wet year (Figure 5), but this relationship was likely influenced by the timing of weeks with high cumulative precipitation in midsummer when both peat temperatures (Figure 1) and productivity (Carroll and Crill 1997; Treat and others 2007) are high, favoring increased acetoclastic methanogenesis (Chang and others 2020; Wilson and others 2021) and therefore higher $\delta^{13}C$–CH_4. Furthermore, given the frequency of our $\delta^{13}C$–CH_4 measurements (bi-weekly), we may have missed the interval over which $\delta^{13}C$–CH_4 responded to rainstorms and flooding. Higher-frequency measurements may help resolve the relationship between rainstorms and $\delta^{13}C$–CH_4.

Conclusions

We measured CH_4 emissions and their ^{13}C isotopic composition from a northern temperate fen across two summers with differing precipitation patterns and water table dynamics. We observed that $\delta^{13}C$–CH_4 values shifted more in response to drought and a lowered water table ($\sim 10‰$) than flooding from rainstorms ($\sim 1‰$), suggesting future droughts may have a large influence on the source signature of $\delta^{13}C$–CH_4 from peatlands as precipitation regimes in the mid to northern latitudes become more variable under climate change. Pairing field measurements of CH_4 fluxes with measurements of $\delta^{13}C$–CH_4 indicated that increased CH_4 oxidation reduced CH_4 emissions under drought. Our results were inconclusive regarding what mechanism caused the pulse of high CH_4 emissions we observed after rainstorms, as our manual measurements may not have occurred over the appropriate timescale to capture the response of $\delta^{13}C$–CH_4 to precipitation events. Higher frequency and/or automated measurements could help resolve this ambiguity, as could experimental efforts simulating rainstorms to aim to capture any shifts in $\delta^{13}C$–CH_4 that occur quickly after flooding occurs. Overall, future investigations of how precipitation impacts peatland CH_4 emissions should continue to incorporate isotopic measurements to help further clarify the physical and biological mechanisms dictating how peatland CH_4 emissions will respond to the changing precipitation regimes expected as climate warming intensifies.

ACKNOWLEDGEMENTS

This work was supported by the New Hampshire Space Grant Consortium Graduate Fellowship, the National Science Foundation MacroSystems Biology Program (EF-1241937), the National Aeronautics and Space Administration Interdisciplinary Research in Earth Science program (NNX17AK10G), the University of New Hampshire Dissertation Year Fellowship, and the University of New Hampshire Hamel Center for Undergraduate Research. The authors would also like to acknowledge Dr. Jack Dibb and Sallie Whitlow for allowing access to Sallie's Fen.

FUNDING

University of New Hampshire, National Science Foundation, EF-1241937, National Aeronautics and Space Administration, NNX17AK10G, New Hampshire Space Grant Consortium.

DATA AVAILABILITY

All CH_4 emissions, $\delta^{13}C$–CH_4, and field-based temperature and water table measurements presented in this manuscript are available at the Zenodo repository under *''Methane Fluxes and 13C-CH4 from a Northern Temperate Peatland''* (https://doi.org/10.5281/zenodo.7549224). Precipitation data used in this study were retrieved from the NOAA National Centers for Environmental Information (https://www.climate.gov/maps-data/dataset/past-weather-zip-code-data-table).

REFERENCES

Avery GB, Shannon RD, White JR, Martens CS, Alperin MJ. 1999. Effect of seasonal changes in the pathways of methanogenesis on the δ^{13}C values of pore water methane in a Michigan peatland. Global Biogeochem Cycles 13:475–484.

Barel JM, Moulia V, Hamard S, Sytiuk A, Jassey VEJ. 2021. Come rain, come shine: peatland carbon dynamics shift under extreme precipitation. Front Environ Sci 9:659953.

Bartoń, K. (2020). MuMIn: multi-model inference. R package version 1.43.17. https://CRAN.R-project.org/package=MuMIn

Bellisario LM, Bubier JL, Moore TR, Chanton JP. 1999. Controls on CH_4 emissions from a northern peatland. Global Biogeochem Cycles 13:81–91.

Breeuwer A, Robroek BJM, Limpens J, Heijmans MMPD, Schouten MGC, Berendse F. 2009. Decreased summer water table depth affects peatland vegetation. Basic Appl Ecol 10:330–339.

Bubier J, Costello A, Moore TR, Roulet NT, Savage K. 1993. Microtopography and methane flux in boreal peatlands, northern Ontario, Canada. Can J Bot 71:1056–1063.

Bubier JL, Moore TR, Bellisario L, Comer NT, Crill PM. 1995. Ecological controls on methane emissions from a Northern Peatland complex in the zone of discontinuous permafrost, Manitoba, Canada. Global Biogeochem Cycles 9:455–470.

Bubier J, Moore T, Savage K, Crill P. 2005. A comparison of methane flux in a boreal landscape between a dry and a wet year. Global Biogeochemical Cycles 19. http://doi.wiley.com/https://doi.org/10.1029/2004GB002351.

Camill P. 1999. Patterns of boreal permafrost peatland vegetation across environmental gradients sensitive to climate warming. Can J Bot 77:13.

Carroll P, Crill P. 1997. Carbon balance of a temperate poor fen. Global Biogeochem Cycles 11:349–356.

Chang K-Y, Riley WJ, Crill PM, Grant RF, Saleska SR. 2020. Hysteretic temperature sensitivity of wetland CH4 fluxes explained by substrate availability and microbial activity. Biogeosciences 17:5849–5860.

Chanton JP. 2005. The effect of gas transport on the isotope signature of methane in wetlands. Organic Geochem 36:753–768.

Chasar L, Chanton JP, Glaser PH, Siegel DI. 2000. Methane concentration and stable isotope distribution as evidence of rhizospheric processes: comparison of a fen and bog in the glacial lake agassiz peatland complex. Ann Botany 86:655–663.

Christensen TR, Ekberg A, Ström L, Mastepanov M, Panikov N, Öquist M, Svensson BH, Nykänen H, Martikainen PJ, Oskarsson H. 2003. Factors controlling large scale variations in methane emissions from wetlands. Geophysical Research Letters 30. http://doi.wiley.com/https://doi.org/10.1029/2002GL016848.

Coleman DD, Risatti JB, Schoell M. 1981. Fractionation of carbon and hydrogen isotopes by methane-oxidizing bacteria. Geochimica Et Cosmochimica Acta 45:1033–1037.

Crill PM, Bartlett KB, Harriss RC, Gorham E, Verry ES, Sebacher DI, Madzar L, Sanner W. 1988. Methane flux from Minnesota Peatlands. Global Biogeochem Cycles 2:371–384.

Dorodnikov M, Marushchak M, Biasi C, Wilmking M. 2013. Effect of microtopography on isotopic composition of methane in porewater and efflux at a boreal peatland. Boreal Environ Res 18:269–279.

Douville H, Raghavan K, Renwick J, Allan RP, Arias PA, Barlow M, Cerezo-Mota R, Cherchi A, Gan TY, Gergis J, Jiang D, Khan A, Pokam Mba W, Rosenfeld D, Tierney J, Zolina O, 2021. Water cycle changes. In: Climate Change 2021: The Physical Science Basis. Contribution of Working Group I to the Sixth Assessment Report of the Intergovernmental Panel on Climate Change [Masson-Delmotte V, Zhai P, Pirani A, Connors SL, Péan C, Berger S, Caud N, Chen Y, Goldfarb L, Gomis MI, Huang M, Leitzell K, Lonnoy E, Matthews JBR, Maycock TK, Waterfield T, Yelekçi O, Yu R, Zhou B (eds.)]. Cambridge University Press.

Dunfield P, Knowles R, Dumont R, Moore T. 1993. Methane production and consumption in temperate and subarctic peat soils: Response to temperature and pH. Soil Biol Biochem 25:321–326.

Fisher RE, France JL, Lowry D, Lanoisellé M, Brownlow R, Pyle JA, Cain M, Warwick N, Skiba UM, Drewer J, Dinsmore KJ, Leeson SR, Bauguitte SJ-B, Wellpott A, O'Shea SJ, Allen G, Gallagher MW, Pitt J, Percival CJ, Bower K, George C, Hayman GD, Aalto T, Lohila A, Aurela M, Laurila T, Crill PM, McCalley CK, Nisbet EG. 2017. Measurement of the ^{13}C isotopic signature of methane emissions from northern European wetlands: Northern Wetland CH_4 Isotopic Signature. Global Biogeochem Cycles 31:605–623.

Frenzel P, Karofeld E. 2000. CH4 emission from a hollow-ridge complex in a raised bog: the role of CH4 production and oxidation. Biogeochemistry 51:91–112.

Frolking S, Crill P. 1994. Climate controls on temporal variability of methane flux from a poor fen in southeastern New Hampshire: measurement and modeling. Global Biogeochem Cycles 8:385–397.

Glaser PH, Chanton JP, Morin P, Rosenberry DO, Siegel DI, Ruud O, Chasar LI, Reeve AS. 2004. Surface deformations as indicators of deep ebullition fluxes in a large northern peatland. Global Biogeochemical Cycles 18.

Goodrich JP, Varner RK, Frolking S, Duncan BN, Crill PM. 2011. High-frequency measurements of methane ebullition over a growing season at a temperate peatland site. Geophysical Research Letters 38.

Greenup AL, Bradford MA, McNamara NP, Ineson P, Lee JA. 2000. The role of Eriophorum vaginatum in CH_4 flux from an ombrotrophic peatland. Plant Soil 227:265–272.

Grolemund G, Wickham H. 2011. Dates and times made easy with lubridate. J Statist Softw 40:1–25.

Heffernan L, Cavaco MA, Bhatia MP, Estop-Aragonés C, Knorr K-H, Olefeldt D. 2022. High peatland methane emissions following permafrost thaw: enhanced acetoclastic methanogenesis during early successional stages. Biogeosciences 19:3051–3071.

Hodgkins SB, Tfaily MM, McCalley CK, Logan TA, Crill PM, Saleska SR, Rich VI, Chanton JP. 2014. Changes in peat chemistry associated with permafrost thaw increase greenhouse gas production. Proc NatL Acad Sci 111:5819–5824.

Hopple AM, Wilson RM, Kolton M, Zalman CA, Chanton JP, Kostka J, Hanson PJ, Keller JK, Bridgham SD. 2020. Massive peatland carbon banks vulnerable to rising temperatures. Nat Commun 11:2373.

Hornibrook ERC, Bowes HL. 2007. Trophic status impacts both the magnitude and stable carbon isotope composition of methane flux from peatlands. Geophys Res Lett 34:L21401.

Huth V, Günther A, Jurasinski G, Glatzel S. 2013. The effect of an exceptionally wet summer on methane effluxes from a 15-year re-wetted fen in north-east Germany. Mires Peat 13:1–7.

Huth V, Hoffmann M, Bereswill S, Zak D, Augustin J. 2018. The climate warming effect of a fen peat meadow with fluctuating water table is reduced by young alder trees. Mires and Peat: 1–18.

Joabsson A, Christensen TR, Wallén B. 1999. Vascular plant controls on methane emissions from northern peatforming wetlands. Trends Ecol Evol 14:385–388.

Keeling CD. 1958. The concentration and isotopic abundances of atmospheric carbon dioxide in rural areas. Geochimica Et Cosmochimica Acta 13:322–334.

Keller JK, Bridgham SD. 2007. Pathways of anaerobic carbon cycling across an ombrotrophic-minerotrophic peatland gradient. Limnol Oceanogr 52:96–107.

Kelly CA, Dise NB, Martens CS. 1992. Temporal variations in the stable carbon isotopic composition of methane emitted from Minnesota peatlands. Global Biogeochem Cycles 6:263–269.

Kettunen A, Kaitala V, Lehtinen A, Lohila A, Alm J, Silvola J, Martikainen PJ. 1999. Methane production and oxidation potentials in relation to water table fluctuations in two boreal mires. Soil Biol Biochem 31:1741–1749.

Knorr KH, Glaser B, Blodau C. 2008a. Fluxes and 13C isotopic composition of dissolved carbon and pathways of methanogenesis in a fen soil exposed to experimental drought. Biogeosciences 5:1457–1473.

Knorr K-H, Oosterwoud MR, Blodau C. 2008b. Experimental drought alters rates of soil respiration and methanogenesis but not carbon exchange in soil of a temperate fen. Soil Biol Biochem 40:1781–1791.

Kolton M, Marks A, Wilson RM, Chanton JP, Kostka JE. 2019. Impact of warming on greenhouse gas production and microbial diversity in anoxic peat from a sphagnum-dominated bog (Grand Rapids, Minnesota, United States). Front Microbiol 10:870.

Kuhn MA, Varner RK, Bastviken D, Crill P, MacIntyre S, Turetsky M, Walter Anthony K, McGuire AD, Olefeldt D. 2021. BAWLD-CH4: a comprehensive dataset of methane fluxes from boreal and arctic ecosystems. Earth Syst Sci Data 13:5151–5189.

Lenth RV. 2021. emmeans: estimated marginal means, aka least-squares means. R package version 1.5.4. https://CRAN.R-project.org/package=emmeans

Moore TR, Dalva M. 1993. The influence of temperature and water table position on carbon dioxide and methane emissions from laboratory columns of peatland soils. J Soil Sci 44:651–664.

National Centers for Environmental Information 2021. Climate data online - daily summaries [data file]. Retrieved from https://www.climate.gov/maps-data/dataset/past-weather-zip-code-data-table

Neumann RB, Moorberg CJ, Lundquist JD, Turner JC, Waldrop MP, McFarland JW, Euskirchen ES, Edgar CW, Turetsky MR. 2019. Warming effects of spring rainfall increase methane emissions from thawing permafrost. Geophys Res Lett 46:1393–1401.

Noyce GL, Varner RK, Bubier JL, Frolking S. 2014. Effect of *Carex rostrata* on seasonal and interannual variability in peatland methane emissions. J Geophys Res Biogeosci 119:24–34.

Olefeldt D, Euskirchen ES, Harden J, Kane E, McGuire AD, Waldrop MP, Turetsky MR. 2017. A decade of boreal rich fen greenhouse gas fluxes in response to natural and experimental water table variability. Global Change Biol 23:2428–2440.

Olson DM, Griffis TJ, Noormets A, Kolka R, Chen J. 2013. Interannual, seasonal, and retrospective analysis of the methane and carbon dioxide budgets of a temperate peatland J Geophys Res Biogeosci 118:226–38.

Pataki DE, Ehleringer JR, Flanagan LB, Yakir D, Bowling DR, Still CJ, Buchmann N, Kaplan JO, Berry JA. 2003. The application and interpretation of Keeling plots in terrestrial carbon cycle research, Global Biogeochem Cycles. 17.

Pedersen TL. 2020. Patchwork: the composer of plots. R package version 1.1.1. https://CRAN.R-project.org/package=patchwork

Peltoniemi K, Laiho R, Juottonen H, Bodrossy L, Kell DK, Minkkinen K, Mäkiranta P, Mehtätalo L, Penttilä T, Siljanen HMP, Tuittila E-S, Tuomivirta T, Fritze H. 2016. Responses of methanogenic and methanotrophic communities to warming in varying moisture regimes of two boreal fens. Soil Biol Biochem 97:144–156.

Perryman, C. R., McCalley, C. K., Ernakovich, J. G., Lamit, L. J., Shorter, J. H., Lilleskov, E., Varner, R. K. 2022. Microtopography matters: Belowground CH_4 cycling regulated by differing microbial processes in peatland hummocks and lawns. J Geophys Res: Biogeosci, 127: e2022JG006948.

Pinheiro J, Bates D, DebRoy S, Sarkar D, R Core Team. 2021. nlme: Linear and Nonlinear Mixed Effects Models. R package version 3.1–153, <URL: https://CRAN.R-project.org/package=nlme>

Popp TJ, Chanton JP, Whiting GJ, Grant N. 1999. Methane stable isotope distribution at a *Carex* dominated fen in north central Alberta. Global Biogeochem Cycles 13:1063–1077.

Radu DD, Duval TP. 2018. Impact of rainfall regime on methane flux from a cool temperate fen depends on vegetation cover. Ecol Eng 114:76–87.

Rey-Sanchez C, Bohrer G, Slater J, Li Y-F, Grau-Andrés R, Hao Y, Rich VI, Davies GM. 2019. The ratio of methanogens to methanotrophs and water-level dynamics drive methane transfer velocity in a temperate kettle-hole peat bog. Biogeosciences 16:3207–31.

Rinne J, Łakomiec P, Vestin P, White JD, Weslien P, Kelly J, Kljun N, Ström L, Klemedtsson L. 2022. Spatial and temporal variation in $\delta^{13}C$ values of methane emitted from a hemiboreal mire: methanogenesis, methanotrophy, and hysteresis. Biogeosciences 19:4331–4349.

Roddy, S. 2014. Vegetation influences on the ebullition of methane in a temperate wetland. [Master's thesis, University of New Hampshire]. UNH Scholars Repository. https://scholars.unh.edu/thesis/993/

Roulet N, Moore T, Bubier J, Lafleur P. 1992. Northern fens: methane flux and climatic change. Tellus B 44:100–105.

Santoni GW, Lee BH, Goodrich JP, Varner RK, Crill PM, McManus JB, Nelson DD, Zahniser MS, Wofsy SC. 2012. Mass fluxes and isofluxes of methane (CH_4) at a New Hampshire fen measured by a continuous wave quantum cascade laser spectrometer. J Geophys Res Biogeosci 117.

Segers R. 1998. Methane production and methane consumption: a review of processes underlying wetland methane fluxes. Biogeochemistry 41:23–51.

Strack M, Waddington JM, Tuittila E-S. 2004. Effect of water table drawdown on northern peatland methane dynamics: Implications for climate change. Global Biogeochem Cycles 18.

Strack M, Kellner E, Waddington JM. 2005. Dynamics of biogenic gas bubbles in peat and their effects on peatland biogeochemistry. Global Biogeochem Cycles 19.

Sundh I, Nilsson M, Granberg G, Svensson BH. 1994. Depth distribution of microbial production and oxidation of methane in northern boreal peatlands. Microb Ecol 27.

Treat CC, Bubier JL, Varner RK, Crill PM. 2007. Timescale dependence of environmental and plant-mediated controls on CH_4 flux in a temperate fen. J Geophys Res Biogeosci 112:G01014.

Treat CC, Bloom AA, Marushchak ME. 2018. Nongrowing season methane emissions-a significant component of annual emissions across northern ecosystems. Global Change Biol 24:3331–3343.

Turetsky MR, Kotowska A, Bubier J, Dise NB, Crill P, Hornibrook ERC, Minkkinen K, Moore TR, Myers-Smith IH, Nykänen H, Olefeldt D, Rinne J, Saarnio S, Shurpali N, Tuittila E-S, Waddington JM, White JR, Wickland KP, Wilmking M. 2014. A synthesis of methane emissions from 71 northern, temperate, and subtropical wetlands. Global Change Biol 20:2183–2197.

Turetsky MR, Treat CC, Waldrop MP, Waddington JM, Harden JW, McGuire AD. 2008. Short-term response of methane fluxes and methanogen activity to water table and soil warming manipulations in an Alaskan peatland. J Geophys Res. 113:G00A10.

Waddington JM, Roulet NT, Swanson RV. 1996. Water table control of CH_4 emission enhancement by vascular plants in boreal peatlands. J Geophys Res 101:22775–22785.

Waddington JM, Morris PJ, Kettridge N, Granath G, Thompson DK, Moore PA. 2015. Hydrological feedbacks in northern peatlands. Ecohydrology 8:113–127.

White JR, Shannon RD, Weltzin JF, Pastor J, Bridgham SD. 2008. Effects of soil warming and drying on methane cycling in a northern peatland mesocosm study. J Geophys Res 113:G00A06.

Whiticar MJ. 1999. Carbon and hydrogen isotope systematics of bacterial formation and oxidation of methane. Chemical Geology 161:291–314.

Whiting GJ, Chanton JP. 1993. Primary production control of methane emission from wetlands. Nature 364:794–795.

Wickham H. 2016. ggplot2: Elegant Graphics for Data Analysis. New York: Springer-Verlag.

Wickham H, François R, Henry L, and Müller K, 2021. dplyr: a grammar of data manipulation. R package version 1.0.5. https://CRAN.R-project.org/package=dplyr

Wilson RM, Tfaily MM, Kolton M, Johnston ER, Petro C, Zalman CA, Hanson PJ, Heyman HM, Kyle JE, Hoyt DW, Eder EK, Purvine SO, Kolka RK, Sebestyen SD, Griffiths NA, Schadt CW, Keller JK, Bridgham SD, Chanton JP, Kostka JE. 2021. Soil metabolome response to whole-ecosystem warming at the spruce and peatland responses under changing environments experiment. Proc Natl Acad Sci USA 118:e2004192118.

Yrjälä K, Tuomivirta T, Juottonen H, Putkinen A, Lappi K, Tuittila E-S, Penttilä T, Minkkinen K, Laine J, Peltoniemi K, Fritze H. 2011. CH4 production and oxidation processes in a boreal fen ecosystem after long-term water table drawdown. Global Change Biology 17:1311–1320.

Yu ZC. 2012. Northern peatland carbon stocks and dynamics: a review. Biogeosciences 9:4071–4085.